



# Numerical Simulation of Two-phase Flow and Heat Transfer Phenomenon in Wickless Heat Pipe

Behrouz Ranjbar

MSc in Mechanical Engineering - Energy Conversion, Torbat Heydarieh Sugar Production Engineer, Azad Mashhad, Torbat Heydarieh, Iran.

**Abstract:** *In recent years, there has been increased tendency toward using heat pipe technology in order to recover heat, save energy and prevent loss in various engineering applications. Heat pipes have important role in many industrial applications, especially in heat exchangers' function improvement and energy saving. In this study, a comprehensive modelling has been conducted for the numerical simulation of the details of two-phase flow and heat transfer phenomenon in wickless heat pipe (Thermosiphon) so that these details cannot be observed in laboratory experiments. Water has been chosen as the fluid and the Volume of Fluid (VOF) of ANSYS FLUENT software is used to model the two phase of water and vapor in thermosiphon. Boiling and condensation (phase transformation) processes in thermosiphon are modelled by coding and adding an UFD code to the FLUENT software. Then, the simulation results are compared to the experimental measurements with the same parameters. Comparison of the results showed that the current modelling in simulation of the heat and mass transfer phenomenon in thermosiphon was successful, and there is good consistency between the temperature profile prediction results by using simulation process and laboratory results. Also, the effect of temperature change and heat input in different times on the thermosiphon operation is studied and the changes of condensed liquid layer on the thermosiphon wall were considered.*

**Keywords:** *Heat Pipe, Heat Exchangers, Heat and Mass Transfer*

## INTRODUCTION

Heat pipe is a two-phase heat transfer device with effective heat transfer rate through fluid evaporation and condensation in a cycle, in a sealed compartment. Wickless heat pipe or two-phase closed thermosiphon is dependent on the gravitational force in order to return the operating fluid to the evaporator.

Heat pipe is an excellent heat conduction device for heat transfer from one part to another. They are mostly recognized as the heat superconductors due to their high heat transfer capacity without losing the heat. Heat transfer rate in thermosiphons is about 1000 times higher than the heat transfer rate in solids with the same dimensions (solid rod and simple blade), which is due to their thermo-physical properties. In this device, one side of the heat pipe (or tube) is filled with an operating fluid. Heat is applied to this side and the fluid is evaporated. The vapor comes to the other side of the pipe, which is cooler, and the liquid is condensed and the heat is released. A simple heat pipe is necessarily composed of a metallic tube (a sealed aluminum or copper compartment that its inner surface has capillary wick materials), which is usually coated with wick and is filled with operating fluid. The heat pipe is like a thermosiphon. The difference between heat pipe and thermosiphon is its capability of heat transfer in the opposite direction of gravitational force with evaporation-condensation cycle using porous capillaries that are like wick s. The wick provides the capillary driving force for restoration of the condensed liquid to the evaporator. The type and quality of the wick

usually defines the heat pipe performance, so it's the heart of the device. Various types of wick s are used according to heat pipe applications.

Wu et.al (2014), studied the effect of wick grooves number on the heat transfer performance of the heat pipe. In this paper, the effect of vapor section increase (zero percent [8 grooves] to 100 percent [16 grooves]) on the heat pipe performance was studied. The results showed that the increase of the wick grooves up to an optimum amount and the increase of vapor section results in the performance increase. The vapor section of 75 percent (14 grooves) has the lowest thermal resistance and in comparison with 8 grooves increases the performance up to 60 percent. This paper presents the 12 grooves as the optimum number of grooves. Chen et. al., (2014) investigated the flat plate heat pipe (FPHP) performance with various filling ratios. Acetone was selected as the operating fluid and according to the results, the liquid filling ratio of 25 percent showed the best thermal performance. In return, improper vacuum and leak greatly reduced the maximum thermal conductivity.

Wu et. al., (2014) studied the effect of thickness of two layer wick on the LHP heat transfer performance. The outer layer of the wick was two-pore layer and the inner layer was single-pore layer. The outer layer lets the passage of the vapor and the inner layer creates the capillary force. This wick type structure reduces the wick strength and vapor release problem while using single-pore wick. Changing the two layered wick thickness ratio increases the heat pipe performance. The higher thickness ratio is related to more two-pore wick and lower thickness ratio is related to more single-pore wick. Alawi et al., (2014) investigated the heat transfer and nanofluids current characteristics in heat pipes. Nanoparticles suspension resulted in the increase of the operating fluid thermal conductivity because the conductivity of solids are higher than liquids. Schampheleire and his coworkers (2015) investigated the small diameter fibers as wick s for capillary force of the heat pipe in the laboratory. The water/copper heat pipe with small diameter fibers and three types of fibrous, screen meshed and porous powder wick s in two direction of counter-gravity and in the aligned with gravity was studied. In the aligned with gravity condition, the screen meshed wick is better than fibrous and porous powder wick s due to its higher permeability and higher capability of operating fluid distribution around the wick. In the counter-gravity condition, the fibrous and screen meshed wick s act equally and both of them, because of small diameter and creation of higher and fine capillary channels, has lower thermal resistance compared to porous powder wick. Kumaresan et al., (2014) has carried out a comparative study on the transfer characteristics of screen meshed and porous heat transfer pipes using CuO/DI water nanofluid. In this paper, the experimental studies has been carried out in order to investigate the thermal performance comparison, surface temperature distribution change, effective thermal resistance and conductivity of screen meshed and porous wick with fluid change, slope angle and heat input parameters. The results showed that maximum surface temperature decrease for porous wick is in the 45° slope and is in the 60° slope for screen meshed with 1% concentration of CuO/DI Water for both types of wick s. The reduction in porous wick thermal resistance was 13.92 percent higher than screen meshed wick. For both of the wick s, the heat input was in the range of 10-160 W, the operating fluid was demineralized water with demineralized water/ Copper oxide nanofluid and the slope angles varied as 0, 90, 75, 60, 45 and 30 degrees. According to the results and the graphs, it could be deduced that thermal performance of the porous wick is better than screen meshed one. Arab and Ali Abbas (2014) created an analytical model to analyze the operating fluid in the thermal pipe. In this paper, an effective and yet simple method based on dimensional analysis is represented to analyze and modify the thermo-physical properties of the operating fluid and predict the effect of operating fluid modification on the thermal resistance of micro-grooved trapezoid heat pipe. The reduced-order model in this study showed that high thermal conductivity, low surface tension, low latent heat of vaporization, low liquid density and high concentration are the most desirable thermo-physical specifications of the operating fluid in order to improve the thermal resistance. Bander (2014) experimentally investigated the temperature distribution in a closed two phase thermosiphon. Figure 2-14 shows the schematic structure of the test device. The thermosiphon is made of a smooth copper tube with outside diameter of 22 mm, the length of 0.5 m and

wall thickens of 0.9 mm. the evaporator and condenser sections have 0.2 m length each and the adiabatic section has 0.1 m length. The evaporator section is heated using a heater with output power of about 500 W. the operating fluid is water and the filling ratio is about 50% of the evaporator.

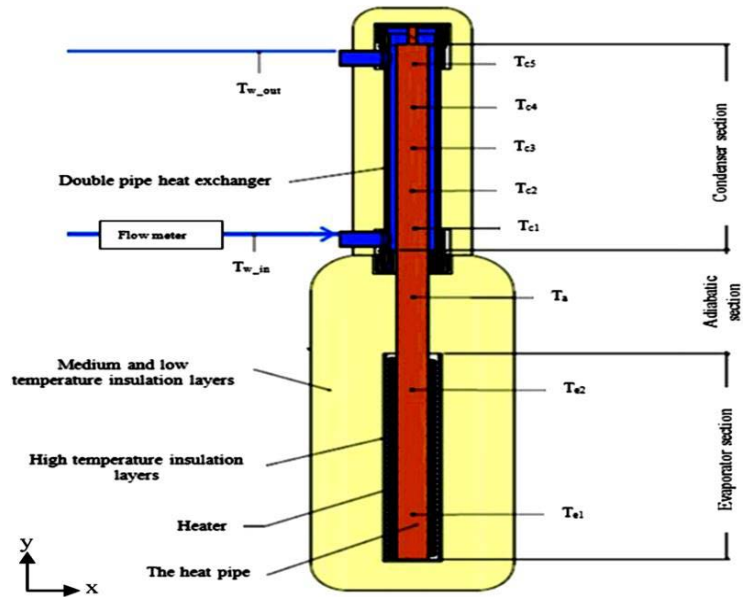


Figure 1: The heat pipe used in this experiment (Bander, 2014).

Figure 1 shows schematic graph of the experiment device, which in evaporator section there are two thermocouples in the distance of 40 mm and 160 mm from the lower part of the evaporator and indexed as  $T_{e1}$  and  $T_{e2}$ , and in adiabatic section  $T_a$  in the center and in condenser section five thermocouples with the indexes from  $T_{c1}$  to  $T_{c5}$  and equal distances. Figure 2 shows the temperature distribution diagram versus the length for various heat inputs.

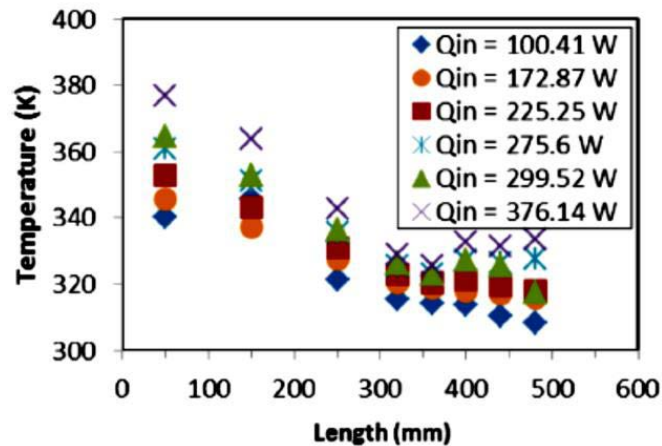


Figure 2: Temperature distribution versus the length for various heat inputs (Bandar, 2014).

Burban (2013) experimentally investigated the Pulsating Heat Pipe (PHP) for hybrid devices. They, in this paper, studied four different operating fluids of water, acetone, methanol and n-pentane in the temperature range of 10-60°C, heat input of 25-550 W, air velocity of 0.25-2 m/s and three slope angles of -45 (condenser over the evaporator), horizontal and -45 (Condenser below the evaporator) degrees. According to the results, it

could be concluded that the water and acetone in high heat inputs and acetone and n-pentane in low heat inputs are suitable for PHP performance improvement.

Due to the researches presented above and considering that the present study is about the thermosiphon heat pipe, so the research done by Bander (2014), which experimentally investigated the temperature distribution in a closed two phase thermosiphon, is selected as the reference research for verification of the results.

**Thermosiphon heat pipe**

Thermosiphon is one of the simplest heat pipes. As shown in Figure 3, a thermosiphon is a vertical wickless heat pipe with a liquid pool in the bottom. A simple thermosiphon is composed of three part like simple heat pipe. As the heat is given to the evaporator, which has the liquid pool, the liquid evaporates. The vapor goes up and passes through the adiabatic section to the condenser, where it releases its latent heat of vaporization and condenses to liquid form. The liquid then is pumped from condenser to the evaporator using gravitational force. In simple thermosiphon, for satisfactory operation, the evaporator should be beneath the condenser, because the liquid return to the evaporator is dependent on the gravitational force. So thermosiphons are ineffective in zero gravity or micro gravity. Thermosiphons are widely used in permafrost protection, cooling of electronic parts and heat exchangers due to their high heat transfer rate, high temperature distribution, their simplicity, reliability and economically affordability. Their limitations in heat transfer like dry-out limit, capillary and flow limits must be considered in design stage of thermosiphons. Dry-out limitation happens in cases where the amount of operating fluid in evaporator is insufficient or the additional heat in evaporator couldn't be eliminated, that causes considerable temperature increase. This is similar to critical thermal flux in boiling pool. The limitation in flow and capillary includes surface shear tension between opposing liquid and vapor currents. The boiling limitation could be found in a thermosiphon with high filling volume and high radial thermal flux in evaporator.

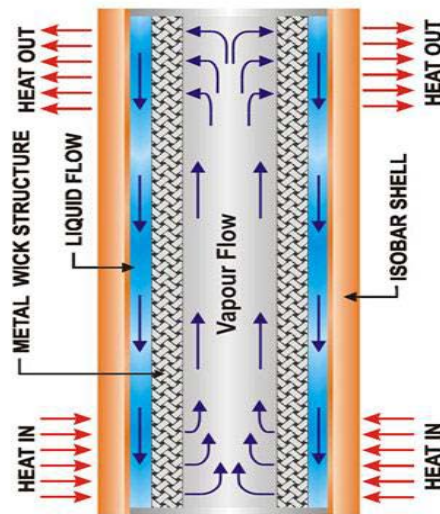


**Figure 3:** Schematics of a thermosiphon (Zohuri, 2011).

**Boiling and condensation**

The transformation from liquid to vapor phase caused by boiling happens, including heat transfer from the surface of the solids. Inversely, vapor condensation (and transformation of the vapor to the liquid) process causes heat transfer to the surface of solid. The latent heat  $h_{fg}$ , surface tension ( $\sigma$ ) between liquid-vapor interface and the density difference between two phases are amongst the parameters that are important in this process. The difference in the densities causes a floatation force that is related to  $g(\rho_l - \rho_v)$ .

**Experimental procedure**

In order to model the thermal thermosiphon, the commercial FLUENT software is used. This software provides the mesh change, completely, and analysis of unstructured mesh currents for complicated geometries. The meshes are produced using GAMBIT software. The type of the meshes that could be produced using GAMBIT are triangular, quadrilateral (for two dimensional geometries), tetrahedral, hexagonal, pyramidal and wedge like (for three dimensional geometries) elements. Moreover, the fluent software allows the operator to improve the network with making the meshes finer or coarser in specific positions.

To model this experiment, a copper heat pipe with 0.5 m length and 0.9 mm thickness is used. The condenser and evaporator sections have 200 mm length and the adiabatic section has 100 mm length that are shown in Figure 4. Two thermocouples of  $T_{e1}$  and  $T_{e2}$  are used to show the temperature in the evaporator section and are positioned in the 40 and 160 mm distance from the below of the section. The other thermocouple  $T_a$  is in the center of the adiabatic section to show the adiabatic section temperature and five thermocouples of  $T_{c1}$  to  $T_{c5}$  are used to show the temperature of condenser part and positioned in equal distances. Figure 5 shows the mesh used in the heat pipe.

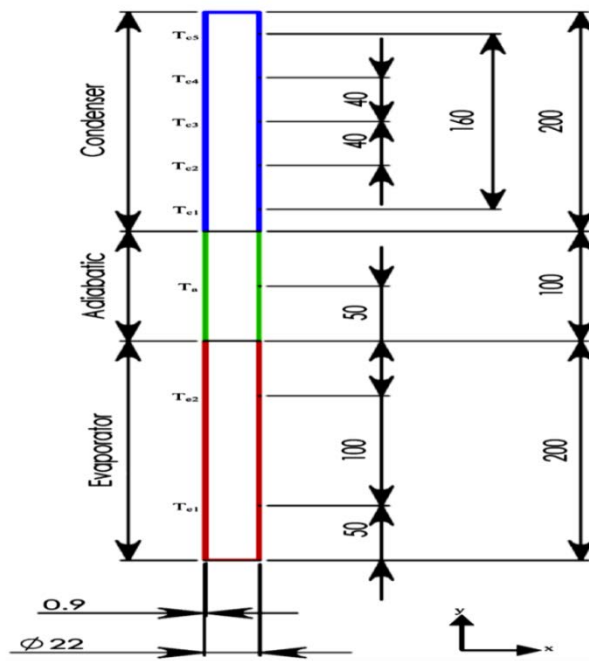


**Figure 4:** The view of the modelled thermosiphon.

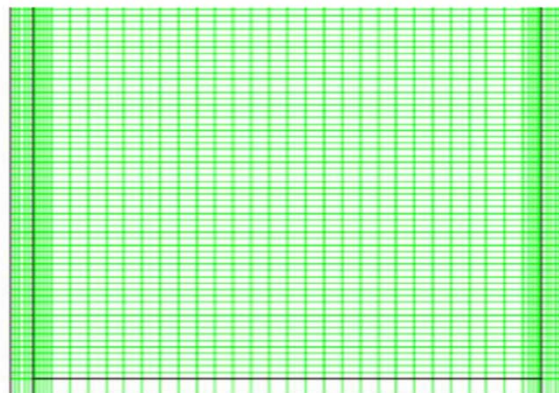


**Figure 5:** Mesh and networking model.

According to the researches carried out by researchers and operation condition of the thermosiphon, the viscosity model is used to solve and the model is laminar flow. In this study, the Volume of Fluid (VOF) model is used to model the two phase flow. The FLUENT software is not capable of modelling the phase transformation in the evaporation and condensation processes. To solve this problem, an UFD code is used to complete the existing FLUENT. This UFD needs the calculations of the heat and mass transfer in evaporation and condensation processes, which is determined using source terms in existing equations specially continuity and energy equations. The source terms are used by De Schepper et al. (2009) to calculate the mass and heat transfer.

**Simulation Results**

The results of the boiling and condensation processes in thermosiphon reaches a semi steady-state condition after a certain period. The temperature distribution in the thermosiphon outer wall for input heats of 172.87 W, 376.14 W is shown in Table 1 and Table 2, respectively. The error percentage is calculated using Equation (1):

$$R_E(\%) = \frac{T_{CFD} - T_{EXP}}{T_{EXP}} \times 100 \tag{1}$$

**Table 1:** The comparison between the experimental (Bandar, 2014) and modelling results for heat input of 172.87 W

Section	Position	T <sub>exp</sub> (K)	T <sub>CFD</sub> (K)	R <sub>E</sub> (%)	T <sub>EXP av</sub> (K)	T <sub>CFD av</sub> (K)	R <sub>E av</sub> (%)
Evaporator	T <sub>e1</sub>	34.755	378.33	9.4	341.6	378.37	10.78
	T <sub>e2</sub>	33.457	378.40	12.14			
Adiabatic	T <sub>a</sub>	32.457	362.41	10.68			10.68
Condenser	T <sub>c1</sub>	32.550	329.54	2.80	318.07	326.96	2.8
	T <sub>c2</sub>	31.855	326.54	2.41			
	T <sub>c3</sub>	31.957	325.95	2.52			
	T <sub>c4</sub>	31.057	325.95	2.71			
	T <sub>c5</sub>	31.95	327.64	3.54			

**Table 2:** The comparison between the experimental (Bandar, 2014) and modelling results for heat input of 376.14 W

Section	Position	T <sub>exp</sub> (K)	T <sub>CFD</sub> (K)	R <sub>E</sub> (%)	T <sub>EXP av</sub> (K)	T <sub>CFD av</sub> (K)	R <sub>E av</sub> (%)
Evaporator	T <sub>e1</sub>	37.756	385.14	2.23	370.2	385.05	4.01
	T <sub>e2</sub>	36.653	384.97	5.86			
Adiabatic	T <sub>a</sub>	34.752	370.11	7.98			7.98
Condenser	T <sub>c1</sub>	32.958	327.12	0.56	330.33	323.96	1.92
	T <sub>c2</sub>	32.555	323.66	0.58			
	T <sub>c3</sub>	33.452	323.15	2.80			
	T <sub>c4</sub>	33.351	323.70	2.61			
	T <sub>c5</sub>	33.353	323.17	3.05			

Eight different positions are considered to show the average temperature of the evaporator, adiabatic and condenser sections. Table 3 shows the average surface temperature for evaporator, adiabatic and condenser sections and also system thermal resistance and relative error between the modelling and experimental results. The simulation results show a trend like experimental results. The average error for average temperature of evaporator, adiabatic and condenser sections are 7.9%, 9.9% and 1.9%, respectively.

**Table 3:** The comparison between the experimental (Bandar, 2014) and modelling results for various heat inputs

Source	Evaporator			Adiabatic			Condenser			Thermal resistance		
	T <sub>e av</sub>	T <sub>e av</sub>	R <sub>E</sub>	T <sub>a</sub>	T <sub>a</sub>	R <sub>E</sub>	T <sub>c av</sub>	T <sub>c av</sub>	R <sub>E</sub>	R <sub>EXP</sub>	R <sub>CFD</sub>	
	EXP	CFD		EXP	CFD		EXP	CFD				
	K	K	%	K	K	%	K	K	%	K/W	K/W	
	343	376.18	9.67	321.25	363.25	13.07	312.412	328.35	5.10	0.3046	0.4763	
	341.6	378.37	10.76	372.45	362.41	10.68	318.7	326.96	2.80	0.1361	0.2974	
	348.1	379.92	9.14	331.05	364.94	10.24	320.55	323.47	0.91	0.1223	0.2506	
	356.1	381.6	7.16	335.55	365.62	8.96	325.95	327.36	0.43	0.1094	0.1967	
	358.75	382.41	6.60	336.25	365.46	8.69	323.91	324.81	0.28	0.1163	0.1923	
	370.2	385.06	4.01	342.75	370.11	7.98	330.33	323.96	1.93	0.1060	0.1624	
Average relative error			7.89				9.94				1.91	

Figure 6 shows experimental and simulation results of external surface temperature distribution in the length of thermosiphon versus various heat inputs. The distance of 0 to 200 mm represents the evaporator section, the distance of 200 to 300 mm represents the adiabatic section and the distance of 300 to 500 mm represents the condenser section. The predicted temperature in the evaporator section has deviation with experimental results, which is due to a continuous heat consideration in the evaporator section. So that in the experiment, a wired heater is wrapped around the evaporator in order to avoid the direct heat application to the top of the evaporator section. The temperature in the condenser section has more consistency with experimental results. Temperature increase in the adiabatic section is due to the axial conduction heat transfer.

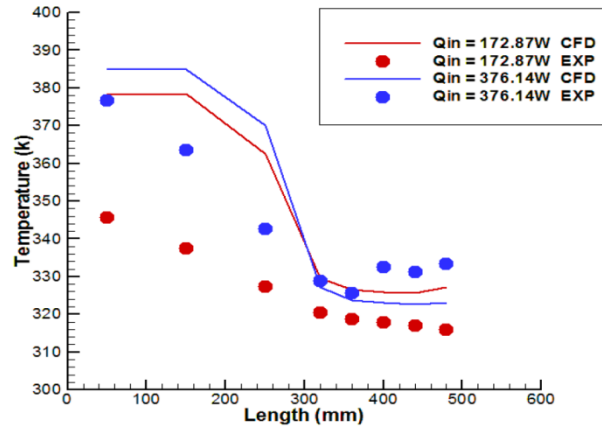


**Figure 6:** The comparison between experimental (Bandar, 2014) and modelling temperature for various heat inputs.

- **Closed two phase thermosiphon performance**

The total heat transfer could be defined as follows:

$$\dot{Q} = \frac{\Delta T}{R} \tag{2}$$

Therefore, the effective thermal resistance of thermosiphon is calculated using the following equation:

$$R_{CFD} = \frac{T_{e\ av\ CFD} - T_{c\ av\ CFD}}{Q_{in}} \tag{3}$$

In the Equation (3) the  $T_{e,ac,CFD}$  and  $T_{c,av,CFD}$  are the temperature of the evaporator and condenser, respectively and the  $Q_{in}$  is the heat input. Different heat inputs are used to investigate the thermosiphon closed two phase performance. Figure 7 shows that the predicted thermal resistance has good consistency with experimental results. As the heat input increases, the thermal resistance decreases. For high heat inputs, the thermal resistance remains relatively independent of heat input. For low heat inputs, the thermal resistance tends to increase. In summary, the results of the simulation is capable of showing the thermosiphon performance variation for various heat inputs.

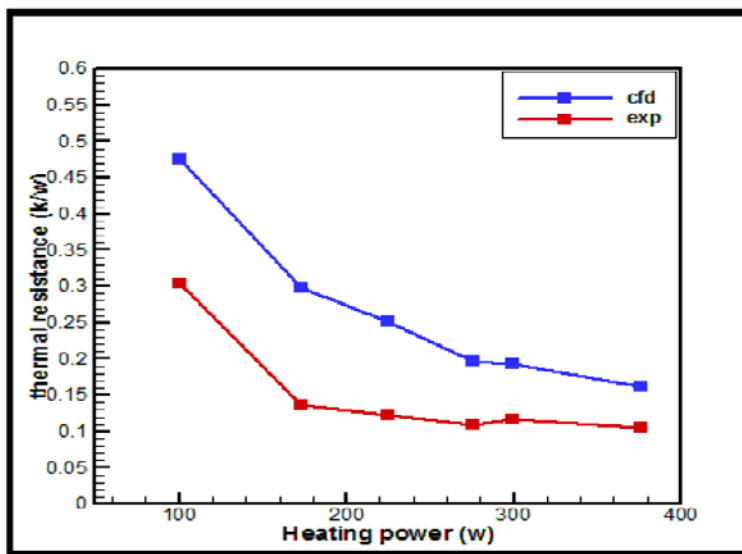


**Figure 7:** The relationship between thermal resistance and heat input.

Figure 8 and Figure 9 show the pool boiling volume ratio contours in the evaporator and condensed liquid film on the condenser in different times. The red color shows the existence of the vapor (volume ratio of the vapor = 1) and the blue color shows the existence of the liquid (vapor volume ratio = 0). In Figure 9 the condensed liquid film in the bottom region of the condenser is focused. In the beginning of the process, the liquid water that has filled half of the evaporator (the other half is filled with vapor) is heated by application of the constant heat input. As shown in Figure 8, when the liquid temperature reaches the boiling temperature, the liquid starts to evaporate and phase transformation happens. Continuous liquid evaporation results in the liquid volume ratio decrease and vapor volume ratio increase. As the liquid evaporates, the bubbles are formed and are transferred to the top section of the liquid water.

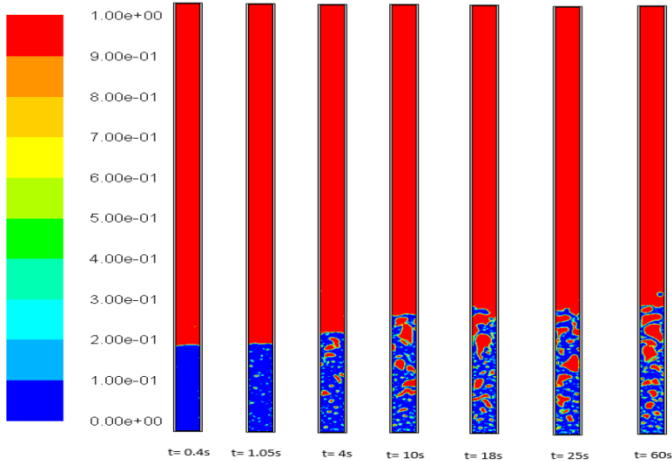


Figure 8: Pool boiling volume ratio contours in the length of thermosiphon in various times.

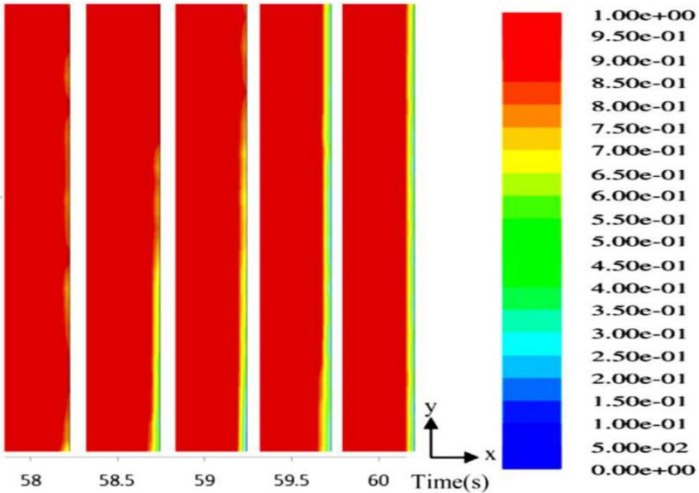


Figure 9: Condensed liquid volume ratio contours in the bottom region of the condenser in various times.

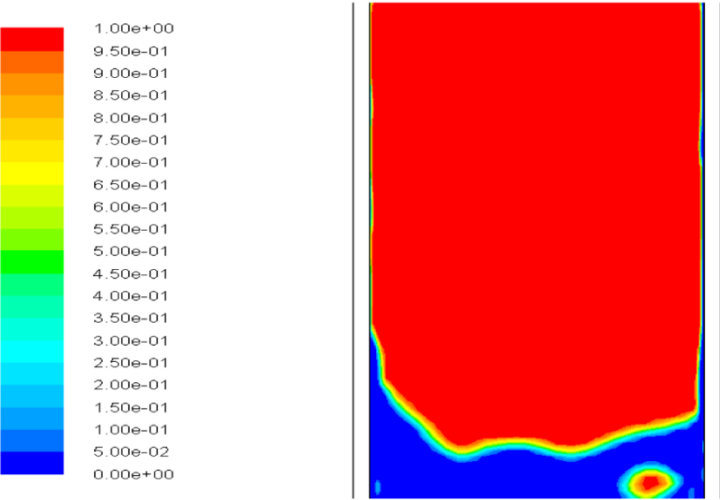
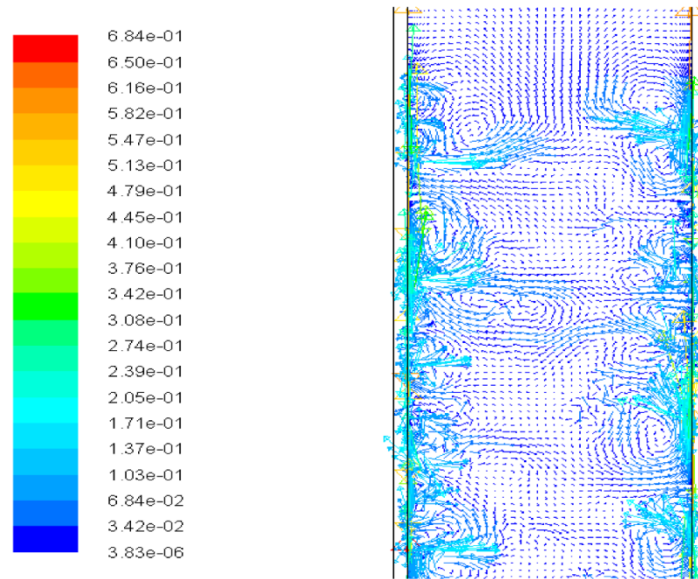


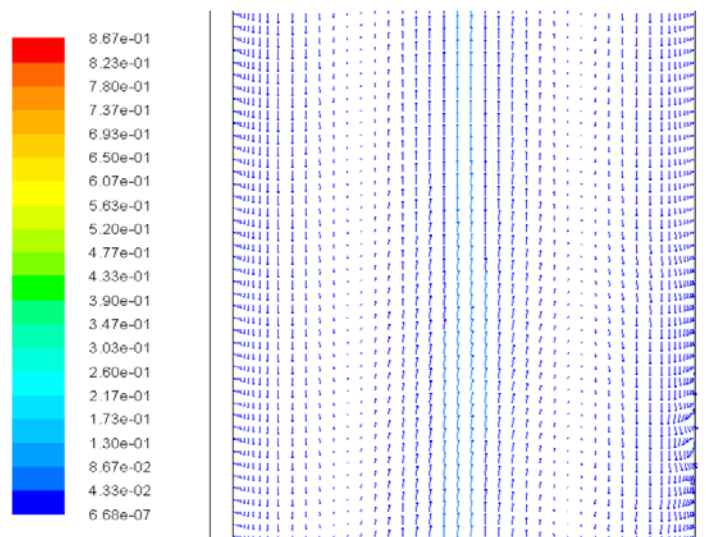
Figure 10: The formation of the condensed liquid.

In the continuation of the process, the saturated vapor is transferred to the upper section of the condenser. As the vapor reaches the condenser wall, it condenses and forms a condensed layer on the cold wall that is shown in Figure 10. This film then goes back to the evaporator section and charges the liquid pool.

Figure 11 and Figure 12 show the velocity vectors. In the evaporator section, since we have a relatively slow liquid pool the velocity vectors are small and as we proceed in the evaporator the vector of vapor velocity sizes increase. In Figure 11 the formation of the whirlpools are because of density change and floatation forces. In Figure 12, in the center, the vectors are upward and in the surrounding of the cooled vapor the vectors are downward and stuck to the wall of the condensed film which moves toward the bottom due to gravitational forces.

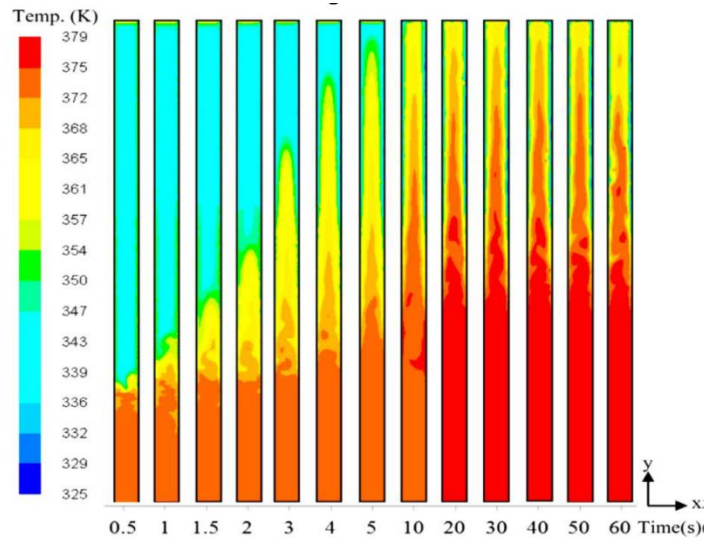


**Figure 11:** Liquid velocity vector, the creation of the whirlpools due to density change and floatation forces.



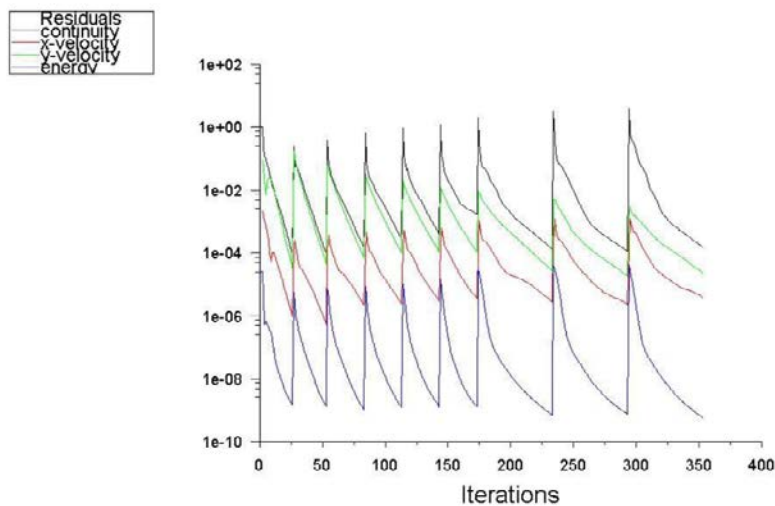
**Figure 12:** The velocity vectors in the vapor region.

Figure 13 shows the temperature contours in the operation of the thermosiphon for input power of 172.87 W. in the beginning, due to the power of heat input, the temperature in the evaporator increases (0.5 s and 1 s). When the evaporator temperature reaches the boiling temperature, the phase transformation starts and the high temperature portion in evaporator increases because of vapor movement toward the upper section (1.5 s to 3 s). As the heat power in the evaporator continues, the vapor flows in the adiabatic and condenser sections (4 s and 5 s). Then, a high temperature region appears in this section due to vapor arrival to the condenser section (10 s). The temperature of the top of the condenser decreases due to condensation of vapor to liquid and the condensed liquid returns to the evaporator because of gravitational forces. The above-mentioned cycle describes the heat transfer process in a thermosiphon operation. After that, the temperature distribution in a thermosiphon reaches a steady-state condition (30 s to 60 s).



**Figure 13:** Temperature contours in different times (in seconds).

Figure 14 shows the convergence diagrams. According to the defined value for the remained convergence, the convergence trend in each time steps (0.0005 s) for continuity equations, velocity and energy are shown. This must be paid attention for transient problems that in the specified time steps the problem should be converged.



**Figure 14:** The convergence diagrams.

## Conclusion

In the present study, the effect of various heat inputs from 100.41 W to 376.14 W was investigated on the thermosiphon performance. The average surface temperature in the length of the thermosiphon is compared to the experimental results in the same condition and the results show that predicted results are in good consistency with experimental ones. The thermal performance of the thermosiphon in various heat powers are specified with effective total thermal resistance and it could be deduced that the increase of the heat input higher than 172 W improves the thermosiphon performance.

## Reference

1. Alawi OA, Sidik NAC, Mohammed HA, Syahrullail S. Fluid flow and heat transfer characteristics of nanofluids in heat pipes: A review. Elsevier. International communications in heat and mass transfer 2014 May: 50–62.
2. Arab M, Abbas A. A model-based approach for analysis of working fluids in heat pipes. Elsevier. Journal of applied thermal engineering. 2014 August. 749-61.
3. Bandar Fadhl LCW, Hussam Jouhara. Experimental investigation of the temperature distribution in a two-phase closed thermosyphon. Elsevier. 2014 June: 122-131.
4. Burban G, Ayel V, Alexandre A, Lagonotte P, Bertin Y, Romestant C. Experimental investigation of a pulsating heat pipe for hybrid vehicle applications. Elsevier. Journal of Applied Thermal Engineering. 2013 June: 94-103.
5. Chen J-S, Chou J-H. Cooling performance of flat plate heat pipes with different liquid filling ratios. Elsevier. International Journal of Heat and Mass Transfer 2014 July: 874–82.
6. De Schepper S.C.K., Heynderickx G.J., Marin G.B., Modeling the evaporation of a hydrocarbon feedstock in the convection section of a steam cracker, Computers & Chemical Engineering 33 (1) (2009) 122–132.
7. Kumaresan G, Venkatachalapathy S, Asirvatham LG, Wongwises S. Comparative study on heat transfer characteristics of sintered and mesh wick heat pipes using CuO nanofluids. Elsevier. International journal of heat and mass transfer. 2014 August: 208–15.
8. Schampheleire SD, Kerpel KD, Deruyter T, Jaeger PD. Experimental study of small diameter fibres as wick material for capillary-driven heat pipes. Elsevier. Journal of applied thermal engineering. 2015 December.258-67.
9. Wu S-C, Wang D, Chen Y-M. Investigating the effect of double-layer wick thickness ratio on heat transfer performance of loop heat pipe. Journal of applied thermal engineering. 2014 July: 292- 8.
10. Wu SC, Wang D, Gao JH, Huang ZY, Chen YM. Effect of the number of grooves on a wick's surface on the heat transfer performance of loop heat pipe. Elsevier. Journal of applied thermal engineering 2014 June. 371-7.
11. Zohuri B. Heat Pipe Design and Technology. New York: Taylor & Francis Group; 2011.